

PAPER

Investigation on surface roughness of ultrasonic assisted vapour smoothing of acrylonitrile butadiene styrene printed sample

To cite this article: Shajahan Maidin *et al* 2024 *Eng. Res. Express* **6** 025402

View the [article online](#) for updates and enhancements.

You may also like

- [Microstructure and mechanical properties of ultrasonic assisted laser cladding \$\text{Al}_2\text{O}_3\$ - \$\text{ZrO}_2\$ ceramic coating](#)
Yuling Wang, Cheng Li, Fulin Jiang et al.
- [Influence of \$\text{TiO}_2\$ and MWCNT nanoparticles dispersion on microstructure and mechanical properties of Al6061 matrix hybrid nanocomposites](#)
Sourabh Kumar Soni and Benedict Thomas
- [Experimental investigation of damage formation and material removal in ultrasonic assisted grinding of RBSiC](#)
Jinting Liu, Renke Kang, Zhigang Dong et al.

Engineering Research Express



PAPER

Investigation on surface roughness of ultrasonic assisted vapour smoothing of acrylonitrile butadiene styrene printed sample

Shajahan Maidin¹, Thavinnesh Kumar Rajendran¹, Mohd Afiq Shahrum¹, Mohd Fitri Mohd Norddin¹, Shafinaz Ismail¹  and Mohd Kamarulnizam²

¹ Faculty of Industrial & Manufacturing Technology & Engineering, Universiti Teknikal Malaysia Melaka, Hang Tuah Jaya, 76100 Durian Tunggal, Melaka, Malaysia

² Esra Energy Resources Sdn Bhd, 8, Jalan Besi 1/2, Kawasan Perindustrian Sungai Purun, 43500, Semenyih, Selangor, Malaysia

E-mail: shajahan@utem.edu.my

Keywords: additive manufacturing, fused deposition modelling, ultrasonic vapour smoothing

Abstract

Additive manufacturing offers many benefits, yet it is confronted with the challenge of rough surfaces resulting from the appearance of seam lines on the printed parts due to the layer-by-layer printing process. This study investigates the effect of ultrasonic-assisted vapor smoothing on the surface roughness of 3D-printed ABS samples. The ABS samples were printed with an open-source FDM printer. The vapour smoothing process was conducted by applying acetone and altering the ultrasonic frequencies and times to 0 kHz, 10 kHz, and 20 kHz for the frequencies and 10 min, 20 min, and 30 min for the times. The surface roughness measurements were performed using a Mitutoyo SJ-301 surface roughness tester. The findings demonstrated enhancements in the quality of the surface, reduction in the visibility of layer lines, and improved surface smoothness for all the samples. From the ANOVA analysis, the average value of Ra for 30 kHz frequency is 2.57 μm , which is better than 3.19 μm for 10 kHz frequency. The manipulation of ultrasonic frequencies and exposure durations decreased surface roughness parameters, suggesting enhancement of the time to attain smoother surfaces. This work demonstrates the effectiveness of ultrasonic-assisted vapour smoothing as a feasible post-processing technique for enhancing surface quality in 3D-printed ABS-printed parts.

Nomenclature

FDM	Fused Deposition Modeling
CAD	Computer-Aided Design
STL	Standard Triangle Language
ABS	Acrylonitrile Butadiene Styrene
AM	Additive Manufacturing

1. Introduction

Additive manufacturing (AM), known as 3D printing, employs a layer-by-layer approach for constructing various components. It differs from subtractive technologies, which fabricate components by removing material from more extensive source materials. The use of this approach has resulted in a substantial revolution in the domain of manufacturing. According to Calignano [1], AM plays a pivotal role in the third industrial revolution. Due to advances in digital technology, AM requires just a three-dimensional digital model. CAD software like AutoCAD, SolidWorks, and CATIA helps create three-dimensional digital models [2]. Design freedom is one of the key benefits of AM technology. Thus, complicated three-dimensional geometries may be converted into final components in a single step without specialist equipment, moulds, or dies [3–5].

Fused Deposition Modeling (FDM) is an AM technique that utilizes thermoplastic materials to fabricate customized samples with complex structures [6]. Acrylonitrile Butadiene Styrene (ABS), a thermoplastic, is widely used in FDM for 3D printing [7]. 3D-printed ABS components have good impact resistance, uniform dimensions, chemical resistance, and electrical properties. They are used in industrial, automotive, electronics, electrical, and instrument sectors [8]. Heated extrusion nozzles offer filaments for building and reinforcing [9]. After heating until partly liquid, the material is discharged via a hot nozzle. The above approach creates discrete component segments that an x-y motion control system carefully controls. The software produced from the CAD model instructs the nozzle to extrude material along x-y curves [10]. After each layer, the build table moves z-wise by one layer thickness. This displacement helps prepare the next layer.

Although the AM technique exhibits proficiency in fabricating components with sophisticated geometrical configurations, it has challenges. One such limitation arises from the occurrence of a phenomenon known as the 'staircase effect' during the printing process [11, 12]. This effect manifests as visible seam lines between successive layers, forming a rough surface on the printed object. According to Maidin's research in [13], a piezoelectric ultrasonic transducer was employed to establish vibration at the initiation of the printing process. Moreover, varying vibration frequencies are employed. The findings indicate that using ultrasonic-assisted printing techniques leads to a notable reduction in surface roughness, up to a 20% decrease compared to conventional test specimens.

ABS is the most often utilized material in the FDM technique. An acetone-based vapour polishing technique reduces the surface irregularity of an ABS-printed part, especially for FDM processes in which the chemical is heated in an enclosed environment [14]. A chamber is used to heat the solvent, causing chemical vapours to disperse across the particles. Thus, the vapour was capable of condensing and penetrating the ABS surface before completing the polishing of the outer layer. The components' mechanical strength and surface texture can be enhanced by coating them with an additional chemical agent [15]. Vapour polishing is a common technique that involves the application of heated vapour to intricate forms, including medical instruments. Chemical vapor works as a solvent to polish the parts' exterior layer and enhances surface polishing, particularly on ABS components [16]. The study in [15], vapour smoothing with acetone, has been considered for the post-processing of ABS parts, and [17] explores the potential use of acetone as an alternate solvent for finishing ABS components in a controlled environment. Utilizing an acetone vapour bath to treat the ABS 3D-printed components is an exceedingly effective and somewhat hazardous method to produce samples exhibiting a lustrous and sleek surface texture. When the model is subjected to an acetone vapour bath or when acetone is applied to the model's surface using a brush, the surface undergoes a melting process. Acetone vapour is advantageous in preserving intricate details while imparting a polished and lustrous appearance [18].

However, several researchers found that ultrasonic-assisted machines can also improve the surface quality of the ABS printed samples. The piezoelectric transducer on the printing platform was utilized to aid the FDM 3D printer in reducing surface roughness. However, none of the studies on the surface roughness of extruded ABS using ultrasonic and assisted vapour smoothing methods. Therefore, this paper examines the surface roughness of ultrasonic-assisted vapour smoothing on ABS-printed samples. The studies will focus on the effects of varying ultrasound frequencies. A device that utilizes a piezoelectric transducer to generate a high-frequency mechanical vibration in a liquid was used. In the presence of fog or mist, this oscillation causes a highly refined dispersion of droplets. The density of the fog was modulated by manipulating the intensity of the vibrations through a potentiometer. In addition, the utilization of vapor polishing serves to enhance the level of surface smoothness.

2. Methodology

2.1. Sample design

The application of the parametric design technique carries notable importance within this situation. It is suggested that any modifications made to the design characteristics of the product are promptly manifested in all workbenches and views. This attribute ensures that any changes made to a specific design component are consistently applied throughout the entire project, improving accuracy and efficiency within the design process. A decision is made to maintain a straightforward and uncomplicated design to facilitate this investigation. The selected exemplary ABS printed sample is a meticulously crafted 3D rectangular item fabricated using CATIA CAD software. The dimensions of the sample have been determined to be 50 mm x 25 mm x 10 mm, so establishing a precise and controlled framework for studying the effects of surface roughness in the presence of ultrasonic vibration and assisted vapour.

The intentional decision to choose a basic design is a conscious choice. This project aims to shift the focus away from the detailed design details. Instead, it emphasizes the intricate correlation between ultrasonic vibration and vapour treatment in connection to the surface qualities of the ABS printed sample. Opting for a streamlined design facilitates the precise attribution of any observed changes in surface roughness to the

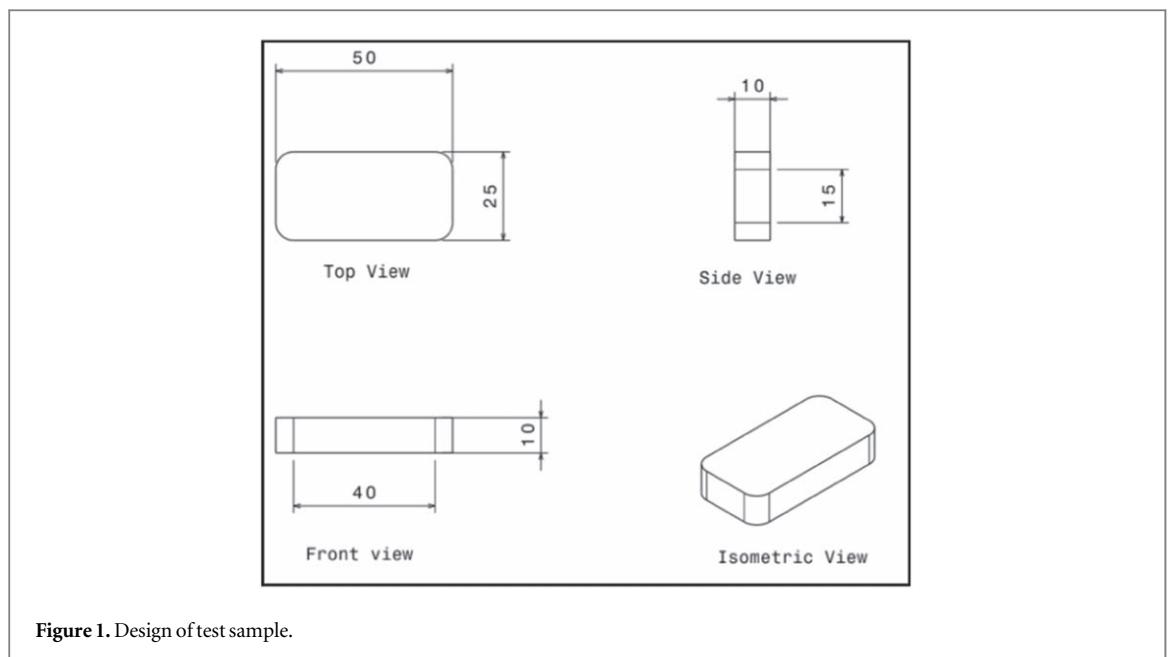


Figure 1. Design of test sample.

Table 1. Parameters of printed sample.

Parameters	Value
Printing Temperature (°C)	230
Bed Temperature (°C)	70°
Layer Thickness	0.2
Infill Percentage	10%
Infill Pattern	Triangle
Printing Speed (mm/s)	60

influence of ultrasonic-assisted vapour smoothing rather than the complexities inherent in the design itself. For a visual representation of the designed test sample, please refer to figure 1 in the project documentation. The presented graphic offers a valuable viewpoint regarding the size and proportions of the ABS sample, successfully demonstrating the deliberate design choice and its alignment with the research objectives.

2.2. Printing parameters

FDM technology is notable for its utilization of specialized 3D printers and industrial-grade thermoplastics, resulting in unparalleled accuracy in the production of components. The layer-by-layer methodology employed by FDM technology, although facilitating the creation of complex geometries, can result in a visual artefact sometimes referred to as the ‘staircase effect.’ As proposed by [15], optimizing process parameters presents a good solution. Improved results were observed for ABS material using an infill of 80%, a layer thickness of 0.5 mm, and a raster angle of 65°. Table 1 presents the recommended settings for ABS filament. In this study, a specified ideal parameter was established before initiating the printing process. This study aims to develop a method of distinguishing the ABS filament used in this project exclusively based on its ultrasonic vibration frequencies during the vapour smoothing process while excluding differentiation based on other parameters. Nevertheless, in this case, the infill percentage was not set at its optimal level since it was decreased to minimize the duration of the printing process.

2.3. Ultrasonic vapour smoothing setup

The experimental procedure applied acetone in an ultrasonic-assisted vapour smoothing method, employing three distinct frequencies (0 kHz, 10 kHz, and 20 kHz) and different durations (10, 20, and 30 min)—this experimental arrangement aimed to produce nine identical ABS test specimens. The ABS samples were contained within a glass jar that was hermetically sealed, functioning as a vapor chamber. The specimens were suspended using a thread firmly fastened to the hook affixed to the jar lid. The injection of acetone into the chamber was performed to create a controlled environment fully saturated with vapours. The experimental setup had ultrasonic transducers adjusted to function at the designated frequencies. The control mechanism

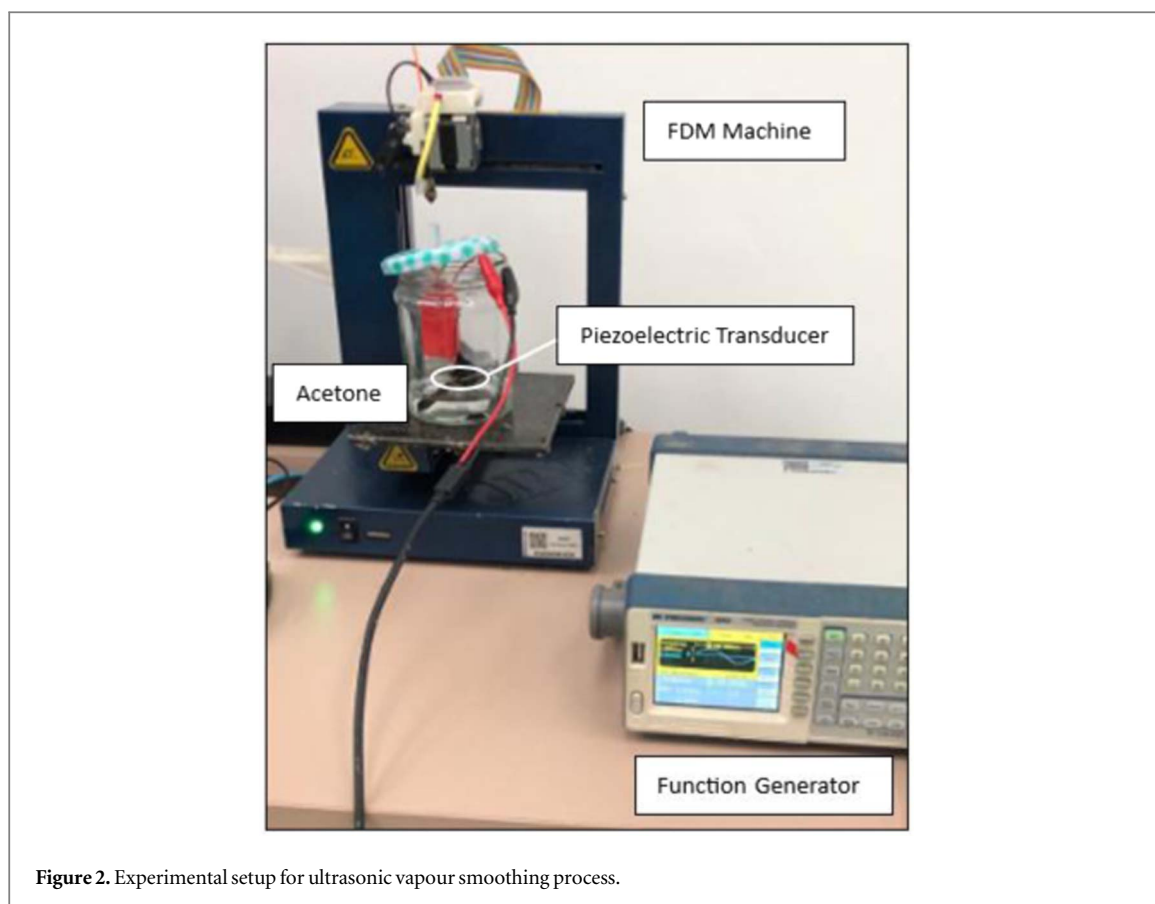


Figure 2. Experimental setup for ultrasonic vapour smoothing process.

Table 2. The cluster for ultrasonic vapor smoothing test sample.

Frequency time	10 min	20 min	30 min
0 kHz	A1	A2	A3
10 kHz	B1	B2	B3
20 kHz	C1	C2	C3

successfully facilitated accurate modification of the ultrasonic frequencies and durations of exposure for each set of samples. The experimental setup for ultrasonic-assisted vapour smoothing is depicted in figure 2.

The nine samples will be grouped into the clusters to which they were assigned once the smoothing process is finished. Cluster A is characterized by samples exhibiting a frequency of 0 kHz, cluster B is characterized by samples showing a frequency of 10 kHz, and cluster C is represented by samples exhibiting a frequency of 20 kHz. Each cluster will consist of three samples that will undergo the process of smoothing at a uniform frequency, albeit with varying periods of exposure. The categorization of test samples based on their assignment to corresponding clusters is presented in table 2.

2.4. Piezoelectric transducer

The piezoelectric transducer is an exceptional device for converting high-frequency electrical energy into mechanical vibrations. This study assumes the role of generating longitudinal vibrations, particularly at frequencies over 20 kHz. The utilization of this ultrasonic transducer is observed in the context of the vapor smoothing technique implemented in the present research.

The strategic placement of the piezoelectric transducer within the vapor smoothing chamber is a crucial element in the overall process of achieving smoothness. The positioning of the treatment has a significant impact on the effectiveness of the smoothing process. In the scope of this study, three specific frequencies, specifically 0 kHz, 10 kHz, and 20 kHz, have been selected as the configurations for the treatment of three separate printed samples positioned within the vapour chamber.

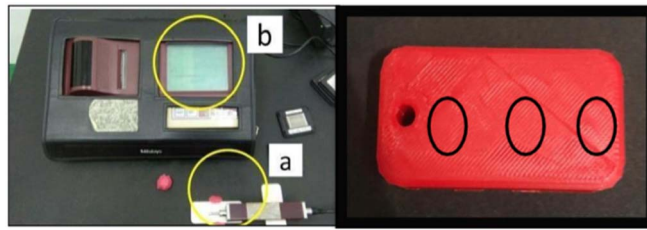


Figure 3. Mitutoyo surfest SJ-301 and the ABS test sample for surface roughness.

Table 3. The specification of the piezoelectric transducer.

Specification of piezoelectric transducer	INC (Piezo system)
Type	Standard quick-mount extension actuator
Weight	2.3 g
Max Voltage	± 90 V
Deflection	$3.6 \mu\text{m}$
Max Amplitude	$10 \mu\text{m}$

The precise design of this system is notable for its effective separation from the surrounding environment. The implementation of isolation measures is of utmost importance, as it serves the dual purpose of mitigating potential disruptions and maintaining optimal and consistent system functioning. To further explore the technical details, table 3 provides a complete overview of the specifications of the piezoelectric transducer. Incorporating specifications provides a more comprehensive comprehension of the equipment's functionalities and aligns with the project's dedication to meticulous documentation.

2.5. Surface roughness test

The evaluation of surface roughness in the surface roughness test involved the utilization of a Mitutoyo Surftest SJ-301 touch probe. Before taking surface roughness measurements, the equipment was calibrated to ensure accuracy. The region's selection for the surface roughness analysis was conducted with great attention.

The touch probe was deliberately positioned on the specimens during the experimental protocol. The measurement was performed thrice at distinct locations on the ABS test sample to confirm the data's trustworthiness. The objective of employing many measurements done at different sites was to obtain a thorough and dependable understanding of the characteristics of the surface. In summary, the average value of the measurements was computed for every printed specimen, offering a comprehensive evaluation of its surface roughness.

Figure 3 in the project documentation provides a graphic representation of the experimental arrangement. The provided diagram depicts the configuration of the Mitutoyo Surftest SJ-301 device and highlights the area on the ABS test specimen that was chosen for quantifying surface roughness. This visual aid enhances the clarity of the experimental setup and underscores the meticulous approach utilized in assessing surface roughness.

2.6. ANOVA

The term 'analysis of variance' appropriately describes the statistical methodology utilized to examine sample data to address research questions [18]. ANOVA modelling offers a feasible method to assess response prediction accuracy by analyzing the interplay between variables using a mathematical framework [19]. Maidin's [20] study utilized analysis of variance (ANOVA) as a statistical method to identify any significant effects on the observed response. A model is deemed statistically significant when the p-value, represented as $\text{prob} > F$, is below 0.05. R_a 's adjusted correlation coefficient evaluates the model's effectiveness [20]. Hence, R^2 and R_a must possess enough magnitudes and exhibit similarity to guarantee enhanced reliability of the best design parameter concerning the analytic model [20].

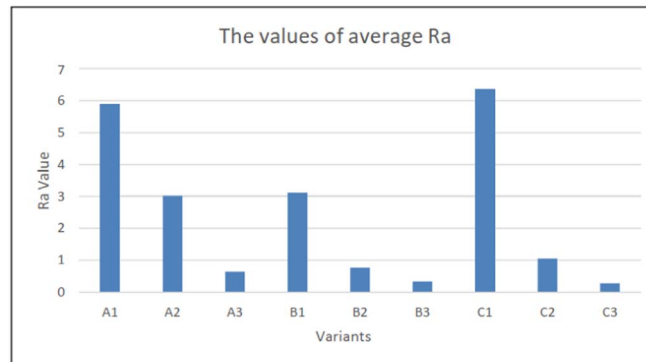


Figure 4. The value of average R_a .

Table 4. The result of surface roughness R_a between three different frequencies and time.

Time Frequency	Ra result		
	10	20	30
0 kHz	A1	A2	A3
	11.78	5.90	1.2
	1.64	2.55	0.3
10 kHz	B1	B2	B3
	4.29	0.61	0.43
	8.40	1.42	0.28
20 kHz	C1	C2	C3
	0.73	0.53	0.28
	0.23	0.34	0.47
	C1	C2	C3
	6.32	1.52	0.47
	5.59	1.14	0.24
	7.20	0.49	0.12

Table 5. The average value of R_a .

Time Frequency	10 min	20 min	30 min
0 kHz	A1	A2	A3
	5.90	3.02	0.64
10 kHz	B1	B2	B3
	3.12	0.76	0.34
20 kHz	C1	C2	C3
	6.37	1.05	0.28

3. Results and discussion

3.1. The value of R_a obtained

Table 4 displays the compiled findings obtained from the surface measurements of the nine test samples. These measurements were conducted using the Mitutoyo Sufest SJ-301 apparatus. The investigation focuses on the frequencies and duration associated with the vapor smoothing process.

On the other hand, table 5 displays the mean values of the surface roughness R_a , which were obtained by three separate measurements for each sample. These two tables will enable the examination of the improvement in surface roughness for ABS printed samples, which is impacted by the manipulation of ultrasonic frequencies and the duration of the vapour smoothing process.

Table 6. ANOVA: two-factor without replication.

Summary		Count	Sum	Average	Variance	
Ultrasonic frequencies	10	3	9.56	3.186667	6.937733	
	20	3	4.22	1.406667	2.245733	
	30	3	7.7	2.566667	10.99723	
Time	0	3	15.39	5.13	3.0853	
	10	3	4.83	1.61	1.5121	
	20	3	1.26	0.42	0.0372	

ANOVA						
Source of variation	SS	df	MS	F	P-value	F crit
Rows	4.8984	2	2.4492	2.2414	0.2223	6.9442
Columns	35.9906	4	17.9953	16.4686	0.0117	6.9442
Error	4.3708	4	1.0927			
Total	45.2598	8				

The graphical representation in figure 4 offers a clear and understandable visualization of the average Ra values associated with clusters A, B, and C. The utilization of this graphical depiction is of utmost significance in enhancing comprehension regarding the evolution of surface roughness in the ABS test specimens. The image has importance due to its capacity to efficiently convey the quantifiable improvements achieved by utilizing the vapour smoothing approach.

An observable pattern emerges after meticulously examining the bars linked to clusters A, B, and C. The Ra value of each cluster demonstrates a consistent drop, suggesting a significant enhancement in surface smoothness. The drop observed in the trajectory indicates that the surface features of the ABS test samples have undergone a notable improvement following the implementation of the smoothing method.

The observed decrease in the bars suggests a reduction in surface faults, unevenness, and imperfections. The observed drop in average Ra values within each cluster provides empirical support for the efficacy of the vapour smoothing procedure in achieving enhanced surface smoothness and polish across all tested samples.

The consistent and ongoing progress observed in vapour smoothing presents encouraging prospects for the practical application of this technique within the AM domain. The finding that all three clusters have decreased average Ra values underscores the robustness and consistency of the methodology. The chart supports our experimental approach's effectiveness and provides a visual tool for statistically evaluating and comparing the effectiveness of the smoothing operation among different sample groups.

3.2. ANOVA: two-factor without replication

Table 6 presents the results of an analysis of variance (ANOVA) performed. The primary emphasis of this analysis centres around the Two-Factor Without Replication design. The ANOVA result was obtained by calculating the mean values of the different ultrasonic frequencies and durations. It would be beneficial to ascertain the frequency and time values that exhibit lower Ra values.

At a frequency of 30 kHz, ultrasonic frequencies demonstrate the lowest average value of Ra. In the above circumstance, the minimum value observed is 1.40 μm at a frequency of 20 kHz, followed by a value of 2.57 μm at 30 kHz. In contrast, the highest attainable value is 3.187 μm when the frequency is 10 kHz. The experiment on ultrasonic-assisted vapour smoothing was conducted multiple times, employing three different sets of clusters: cluster A (with a frequency of 0 kHz), cluster B (with a frequency of 10 kHz), and cluster C (with a frequency of 20 kHz). The experiment about applying smoothing techniques on cluster C was conducted in the third week of the research. There exists a potential for a drop in the concentration of acetone chemical as an outcome.

4. Conclusion

The study investigating the application of ultrasonic-assisted vapour smoothing technology on ABS printed samples has produced noteworthy findings about the surface quality and roughness of the treated samples. Upon visual inspection of the provided samples, it was seen that there was a discernible enhancement in the overall surface aesthetics. The phenomenon was evidenced by a decrease in the perceptibility of layer lines and an overall improvement in the surface's level of smoothness. In addition, the surface roughness analysis yielded numerical measures that enabled the evaluation of the efficacy of the methodology. The study's findings revealed a positive correlation between higher ultrasonic vibration frequencies, namely 20 kHz, and longer exposure durations of 30 min with a notable decrease in surface roughness characteristics. The average roughness (Ra)

demonstrated a decrease in values, indicating the presence of surfaces that possess a higher degree of smoothness.

Nevertheless, it is essential to acknowledge that specific test samples, namely C1 and C2, yielded unforeseen outcomes. The Ra value of these samples should be the lowest compared to other members of their respective clusters. Nevertheless, the results collected reveal a divergent trend. The influence of storage conditions and duration on acetone is a noteworthy contributing factor. The maintenance of acetone concentration is contingent upon using appropriate storage techniques. The potential for reduced acetone concentrations arises when it is stored in containers lacking airtight seals or not primarily intended for chemical storage, as leakage or evaporation may occur.

Regarding the attribute of extended duration, it has been shown that acetone can undergo degradation or chemical conversions. These events may exhibit susceptibility to various variables, including factors such as the presence of light, air, or specific environmental conditions. Consequently, it is plausible for the concentration of acetone to diminish over an extended duration progressively.

Acknowledgments

The authors acknowledge the University Teknikal Malaysia Melaka for awarding the Zamalah Scholarship.

Data availability statement

All data that support the findings of this study are included within the article (and any supplementary files).

ORCID iDs

Shafinaz Ismail  <https://orcid.org/0000-0001-7883-250X>

References

- [1] Calignano F, Galati M, Iuliano L and Minetola P 2019 Design of additively manufactured structures for biomedical applications: a review of the additive manufacturing processes applied to the biomedical sector *Journal of Healthcare Engineering* **2019** 1–6
- [2] Nadhilah I and Ilias B 2022 Automatic Additive Manufacturing Product Generation Through Computer Aided Process Planning Using 3D / 4D / 5D *Doctoral dissertation* Universiti Sains Malaysia
- [3] Bozkurt Y and Karayel E 2021 3D printing technology; methods, biomedical applications, future opportunities, and trends *J. Mater. Res. Technol.* **14** 1430–50
- [4] Diegel O, Nordin A and Motte D 2019 *A Practical Guide to Design for Additive Manufacturing* ed O Diegel et al (Springer) p 226
- [5] Altıparmak S C, Yardley V A, Shi Z and Lin J 2022 Extrusion-based additive manufacturing technologies: state of the art and future perspectives *J. Manuf. Process.* **83** 607–36
- [6] Wang X, Jiang M, Zhou Z, Gou J and Hui D 2017 3D printing of polymer matrix composites: a review and prospective *Composites Part B: Engineering* **110** 442–58
- [7] Ahmad M N, Ishak M R, Mohammad Taha M, Mustapha F, Leman Z, Anak Lukista D D, Irianto and Ghazali I 2022 Application of Taguchi method to optimize the parameter of fused deposition modeling (FDM) using oil palm fiber reinforced thermoplastic composites *Polymers* **14** 2140
- [8] Li G et al 2018 Effect of ultrasonic vibration on mechanical properties of 3D printing non-crystalline and semi-crystalline polymers *Materials* **11** 826
- [9] Gawel T 2020 Review of additive manufacturing methods *Solid State Phenom* **308** 1–20
- [10] Dey A and Yodo N 2019 A Systematic Survey of FDM process parameter optimization and their influence on part characteristics *J. Manuf. Mater. Process.* **3** 64
- [11] Rakshit R, Ghosal A, Paramasivan K, Podder S, Misra D and Panja S C An experimental investigation of surface roughness and print duration on FDM printed polylactic acid (PLA) parts 2022 *Interdisciplinary Research in Technology and Management (IRTM)* **2022** 1–5
- [12] Maidin S, Hayati N M N, Rajendran T K and Muhammad A H 2023 Comparative analysis of acrylonitrile butadiene styrene and polylactic acid samples' mechanical properties printed in vacuum *Additive Manufacturing* **67** 103485
- [13] Maidin S, Abdullah A, Nor Hayati N M, Albaluoshi H and Alkahari R 2022 Application of taguchi method to optimize ultrasonic vibration assisted fused deposition modeling process parameters for surface roughness *J. Teknol.* **84** 125–33
- [14] Chaudhari Aditya A, Godase Akshay M, Jadhav Ravindra S and Abhijit V N 2017 Acetone vapor smoothing: a post-processing method for 3D printed ABS parts *Int. J. Res. Sci. Innov.* **IV** 123–7
- [15] Mishra S B, Acharya E, Banerjee D and Khan M S 2019 An Experimental Investigation of surface roughness of FDM build parts by chemical misting *IOP Conf. Ser. Mater. Sci. Eng.* **653** 012043
- [16] Mazlan S N H, Alkahari M R, Ramli F R, Maidin N A S, Sudin M N and Zolkaply A R 2018 Surface finish and mechanical properties of FDM part after blowing cold vapour treatment *J. Adv. Res. Fluid Mech. Therm. Sci.* **48** 148–55
- [17] Chohan J S, Singh R and Boparai K S 2019 Vapor smoothing process for surface finishing of FDM replicas *Mater. Today Proc.* **26** 173–9
- [18] Khosravani M R, Schüürmann J, Berto F and Reinicke T 2021 On the post-processing of 3d-printed abs parts *Polymers (Basel)* **13** 1–13
- [19] Setting T *Basic ANOVA concepts One-Way ANOVA* **2** 1–6
- [20] Maidin S, Muhammad M K and Pei E 2015 Feasibility study of ultrasonic frequency application on FDM to improve parts surface finish *J. Teknol.* **77** 27–35